High-Temperature Solid-Lubricated Bearing Development—Dry Powder-Lubricated Traction Testing

Hooshang Heshmat*
Mechanical Technology, Inc., Latham, New York 12110

As part of a high-temperature, dry-lubricated bearing technology and lubricant system development program, a high-speed and high-temperature disk-on-disk tribometer was utilized and a matrix of traction data covering a range of loads, speeds, and temperatures was obtained. An experimental investigation of powder-lubricated rolling and sliding contacts for three types of triboparticulates (NiO, TiO_2, and $ZnMoO_2S_2$) was undertaken. The influence of dry triboparticulates on the traction coefficients between two ceramic materials (Si_3N_4 against itself) was investigated. The most important results of this investigation are characteristic curves for the traction coefficient versus the slide/roll ratio with dry powders which are reminiscent of fluids, and the observation that dry powder lubricants lower traction coefficients and wear. Measured tractions are found to be a strong function of powder lubricant type and values decrease with slide-to-roll ratio and load. The data show a weak sensitivity to temperature over the 70°F to 1200°F range.

Nomenclature

CER	=	Si_3N_4, Cercom "pad" improved
E_1, E_2	=	modules of elasticity of disk 1 and disk 2
F_x	=	tractive force in rolling direction
$K162B$	=	TiC cermet with Mo and Ni as a binder
Kyo	=	Si_3N_4, Kyocera
N_A	=	rotational speed of lower disk (disk 1)
N_B	=	rotational speed of upper disk (disk 2)
NBD	=	Si_3N_4, NBD-100
$\%\Delta U$	=	$((U_2 - U_1)/U_1) \times 100$ = percent slip ratio
P_{HZ}	=	Hertz maximum pressure
R_1, R_2	=	outer radius of disk 1 and disk 2
R_{c1}, R_{c2}	=	crown radius of disk 1 and disk 2
RT	=	room temperature $\simeq$ 25°C
Ta	=	ambient temperature
U_1, U_2	=	surface velocity of disk 1 and disk 2
α_1	=	angle of slope at maximum traction (deg)
α_2	=	angle of slope at stable portion of traction curve
$\nu_{1,2}$	=	Poisson's ratio of disk 1 and disk 2
τ_0	=	coefficient of yield shear stress (threshold)
τ_l	=	coefficient of limiting shear stress
τ_T	=	coefficient of thermal limiting shear stress

Introduction

THE need for solid lubricated bearing technology has become increasingly evident with the recent advanced turbine engine initiatives which are aimed at achieving a revolutionary improvement by doubling propulsion capacity. Attaining this performance improvement goal will require the engine bearings to be subjected to increased temperatures, loads, and speeds—a severe operating environment for bearings of the future. The severity of this environment precludes the use of current liquid lubricants, since bearing temperatures are expected to exceed 1000°F and may reach levels as high as 1500°F.

It naturally goes without saying that such an extreme environment precludes the use of liquid lubricant and the most common materials such as VIM-VAR M50 used for aeroengine bearings since their practical operating temperatures are limited to 700–800°F. In Fig. 1, one important characteristic of some potential high temperature cermet and ceramic materials for rolling element bearings is compared. As can be seen from the plots of Fig. 1, under constant applied loads the computed maximum Hertzian stress varies substantially for a given material combination. A group of materials which appears promising for high-temperature bearings is high-performance ceramics. Prominent among them is the hot pressed silicon nitride series (known by their tradenames: Kyocera, NBD-100, Cercom "PAD"), which have been developed during this decade for high-speed and high-temperature rolling element bearings. Despite their many advantages, there are drawbacks with Si_3N_4, including high coefficient of friction ranging from 0.5 to 1.0 or higher, low-tensile strength, low-thermal coefficient of expansion and moderate wear properties in the absence of lubricant. Thus, considerable development effort is needed for the fabrication and application of bearings from these ceramics.

One potential solution to the temperature problem is to use dry triboparticulates (powder lubricants) to minimize bearing friction and wear and to maximize heat dissipation in the bearing's mating surfaces.[1-3] The tribology of powder lubrication's central proposition is that provided the particles

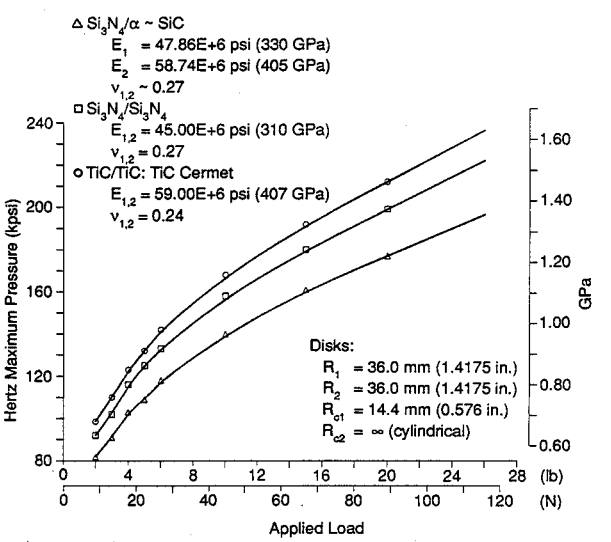

Fig. 1 Contact pressure vs applied load for various material combinations; □ Si_3N_4/α-Sic; △ Si_3N_4/Si_3N_4, ○ TiC/TiC.

Received May 10, 1990; presented as Paper AIAA-90-2047 at the 26th AIAA/SAE/ASME/ASEE Joint Propulsion Conference, Orlando, FL, July 16–18, 1990; revision received Aug. 18, 1990; accepted for publication Sept. 4, 1990.

*Senior Program Manager/Senior Scientist, 968 Albany-Shaker Road.

are small enough, the mechanism and rheodynamics of dry powders acting as lubricants are in many ways similar to the hydrodynamic action of non-Newtonian fluids.[1-4] Thus, an important aspect in the application of dry triboparticulate lubrication is the understanding of frictional force developed in shearing a powder film in a Hertzian contact. Most of the experimental data to date have been obtained from pin-on-disk machines to which the friction forces are measured in pure sliding. Although these data are far from complete, they show that in general the frictional force increases with the sliding speed, up to a peak value and beyond this point an increase in sliding speed causes a decrease in friction.

This paper describes an advanced rolling/sliding tribometer designed to obtain traction data under high speed, loads, and temperatures for both powdered and nonpowdered (dry) conditions. Data are presented for hot pressed, silicon nitride (Si_3N_4) disks (manufactured by Kyocera). The powder lubricants used include nickel oxide, NiO; titanium dioxide, TiO_2 (rutile form); and zinc oxythiomolybdate, $ZnMoO_2S_2$. Surface speeds up to 68 m/s (13,386 ft/min), temperatures from 70 to 1200°F, and slip ratios up to 100% were investigated. Baseline data were obtained for unlubricated conditions and using a synthetic liquid lubricant. The results of baseline data correlated well with other available data for the conditions that are reported here and elsewhere.[5-7]

The powder-lubricated data are analyzed in various ways, however, the lack of previously published data in the literature did not allow for comparison. Although the experimental observations presented in this paper are an extension of considerations and theory developed in an earlier paper by Heshmat, Pinkus, Godet,[1] and Heshmat,[2] the traction data is presented here to provide a data base and guidelines for designers to arrive at reasonable estimates of powder lubricant properties under severe conditions of operation.

Experimental Setup

A schematic of the disk-on-disk tribometer used for conducting tests is presented in Fig. 2. The lower disk, #1, mounted on spindle A, has a plain cylindrical form with a radius of 36 mm. The upper crowned disk #2 on spindle B has a major radius of 36 mm and a crown radius of 14.4 mm. The contact surfaces of the disks were lapped to achieve 0.51 nm or better finish. For the tests, the disks were made from hot pressed Si_3N_4 (from Kyocera). The design methodology and dynamic analysis of this apparatus is given in Ref. 8.

As shown in Fig. 2, Spindle A is rigidly mounted on the base and is driven by a variable-speed electric motor through a quill shaft and flywheel. Spindle B is driven by an integral air turbine. The spindle unit is suspended on a soft spring, but is restrained by hydrostatic bearings. These bearings operate against a vertical member which is integral with the base. The hydrostatic bearings keep the axes of the two spindles parallel but present virtually no resistance to the vertical and small rotational motion of Spindle B. In operation, the disks are loaded by a pneumatic cylinder that pulls down on Spindle B through a load cell. The traction force is measured by a tangential load cell, as shown in Fig. 2, view A-A. An insulated oven enclosure surrounds the two disks to control the environment for high-temperature testing. During the tests, temperatures were monitored by three thermocouples located close to the disks and contact area.

The system for delivering powder lubricants to the inlet zone of the contact is based on a conventional airbrush. A tube from the airbrush nozzle penetrates the oven wall and discharges the dry air/powder mixture approximately 25 mm from the contact zone. The flow rate of the powder was kept constant at about 2 cc/min through these tests. This was done via the use of a commercial airbrush device with regulated dry air supplied at 35 psi. The maximum powder flow on the basis of the possible maximum surface speeds that could be achieved with the existing test rig were calculated to be about 0.23 cc/min (for given maximum film thickness). Then a sufficient amount of powder flow (by tenfold that of required) was directed toward the contact entrance zone to assure the region of lubrication would always be in a flooded condition and starvation phenomena would not enter into the test matrix as an additional parameter. The test powders were obtained from commercially available sources with particular emphasis on their level of purity and particulate average size.

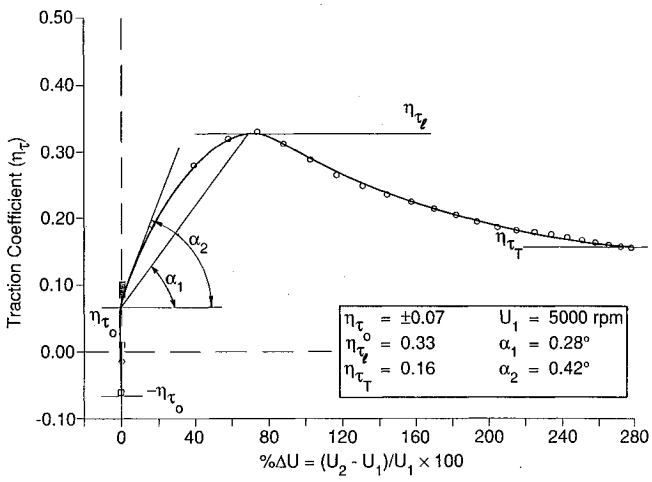

Fig. 3 Definition of traction curve parameters; TiO_2 powder at *RT*, *Wn* = 44.48N, 10 lbs.

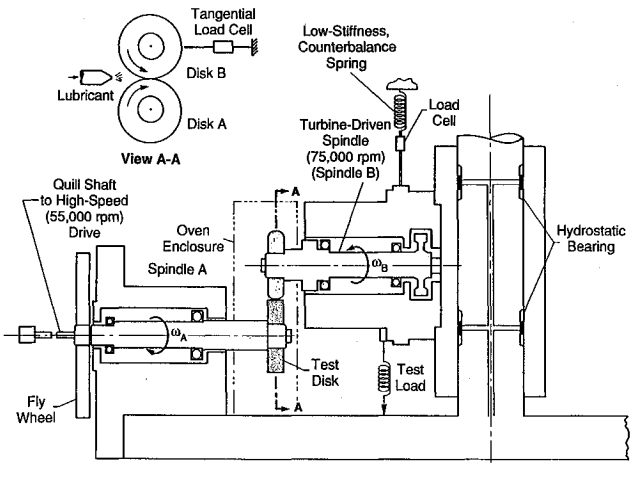

Fig. 2 Extreme environment rolling/sliding traction simulator.

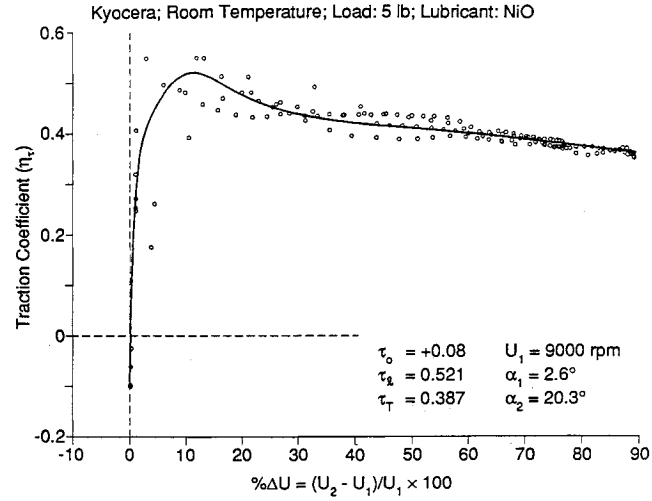

Fig. 4 η_τ vs %ΔU for NiO powder at *RT*, *Wn* = 22.23N.

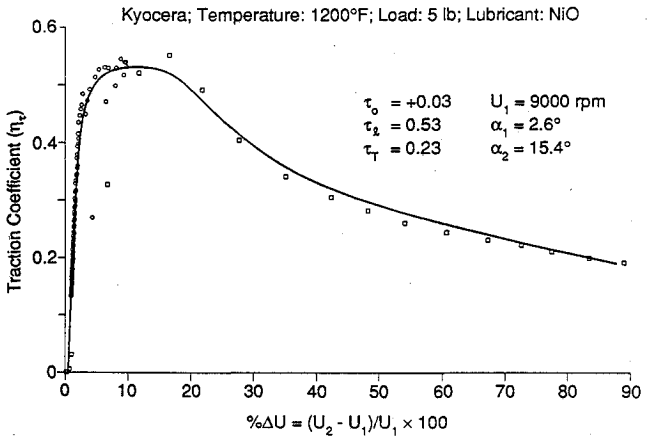

Fig. 5 η_τ vs $\%\Delta U$ for NiO powder at 650°C, Wn = 22.23N.

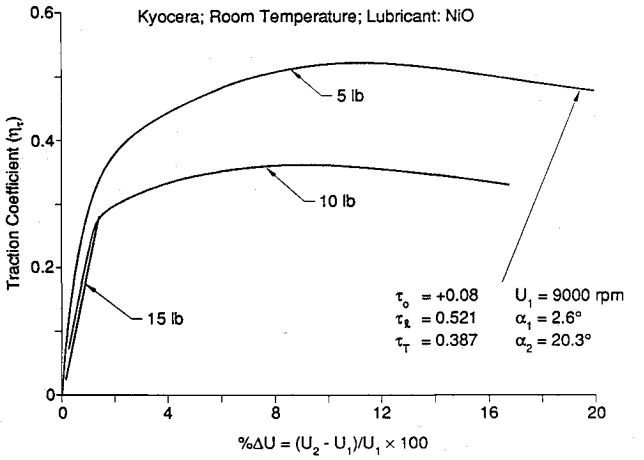

Fig. 6 Traction data for NiO powder at *RT*; Wn = 22.23, 44.48, and 66.72N.

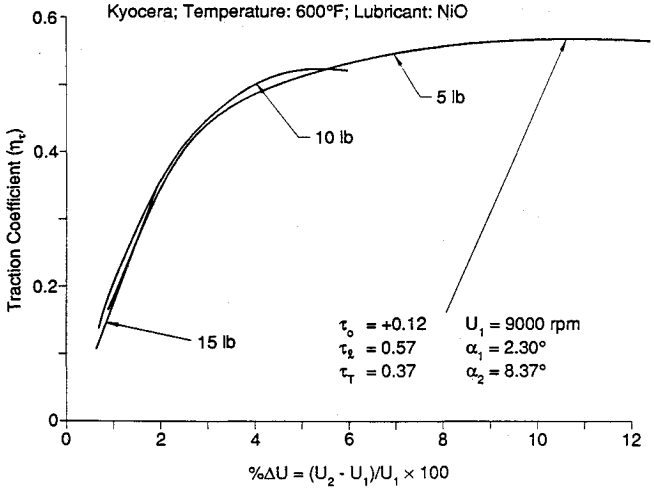

Fig. 7 Traction data for NiO powder at 316°C; Wn = 22.23, 44.48, and 66.72N.

Prior to operation, the suspension spring for Spindle B is adjusted so that the disks are separated from each other by a distance of 90 to 100 μm with no pressure in the loading cylinder. Spindle A (disk #1) is then accelerated to a preselected speed that is maintained throughout the test. Spindle B (disk #2) is then accelerated to a speed higher than that of Spindle A. The traction test is started by applying the load, which brings the disks into contact, and then shutting off the air to the drive turbine. Spindle B subsequently coasts down to a speed lower than that of Spindle A. The sequence of events for each test is carried out automatically by a rig control and data acquisition system based on a PC/AT computer. During coastdown, the speed and traction force are continuously monitored and data are stored for subsequent analysis. During a typical 5- to 6-s coastdown, 1.5 to 2 megabytes of data are recorded and 250 to 300 data points are subsequently extracted from this raw data to produce a traction curve. Some tests were repeated up to eight times in order to verify the repeatability of the traction data.

The triboparticulate size ranged from 0.1 to 10 μm with 99.99% purity for all lubricants, yielding cumulative 50 per cent by weight average particle size of 5.95 μm. Powder lubricants including NiO with a light green color (particles having spheroid shape), TiO_2 with a tan color in rutile form, and zinc oxythiomolybdate with a dark orange color (particles of TiO_2 and $ZnMoO_2S_2$ having irregular shapes with many facets and sharp edges) were tested.

The test load, speed conditions and temperatures were as follows:

W_n: 5 to 15 lbs.

Speeds: N_A = 150 cps; N_B: 150–300 cps

Ta: 22°C–650°C (RT to 1200°F)

For the disk material and geometries, the maximum Hertzian stress as a function of normal load is given in Fig. 1 (Si_3N_4/Si_3N_4 curve).

Traction Data

Traction coefficients η_τ are defined here as the measured tractive force divided by applied normal load W_n and slip rates are defined as the difference between the surface velocities $(U_2 - U_1)$. The traction data are presented in the form of η_τ vs. percent slip ratio, $\%\Delta U$.

For comparison of relative performance, the traction curves were fit. Figure 3 includes some additional data that are valuable in comparing and classifying different traction curves. Data relevant to the characteristics of a particular traction curve such as τ_0, τ_l, τ_T, and others are given with the subsequent plots. Where τ_0, coefficient of yield shear stress—a powder is not likely to flow until the shear exceeds the yield strength of the powder film. In addition to τ_0, a powder film has a limiting shear strength τ_l which is related to the bulk powder property, characteristics, and physical boundary conditions of the tribosurfaces.

As can be seen from Fig. 3, the traction initially increases with increasing slip until the traction coefficient reaches a

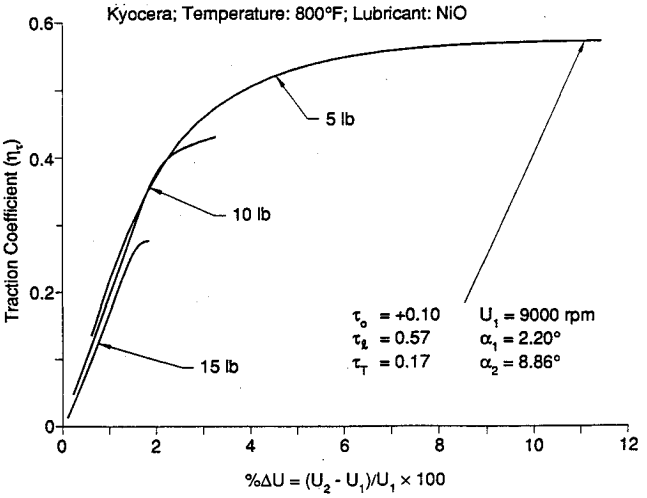

Fig. 8 Traction data for NiO powder at 427°C; Wn = 22.23, 44.48, and 66.72N.

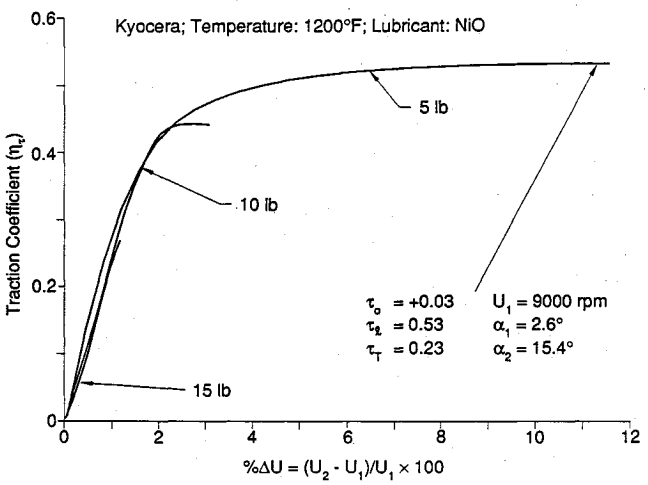

Fig. 9 Traction data for NiO powder at 650°C; *Wn* = 22.23, 44.48, and 66.72N.

value of limiting shear, τ_l, then gradually decreases as slip rate increases. The decrease in traction coefficient beyond τ_l, up to a limiting value of τ_T, is believed to be due to the temperature rise and other tribological phenomena as is evident from traction behavior of liquid lubricants at a higher slip/roll region.[5,6]

The angle of slope at maximum traction and the angle of slope of the stable portion of traction are designated by α_1 and α_2, respectively (Fig. 3). For instance, the smaller the magnitude of α_1, the higher the stable region of the traction curve is and vice versa. The greater the α_2, the higher the ratio of traction force over slip velocities. The traction data are presented here in the following parametric manner:

a) For each powder lubricant the traction data of constant W_n at *RT*, and at maximum test temperature are presented individually.

b) Traction curves are combined for each constant test temperature as a function of the applied load.

For the latter case test data points were omitted from the plots while smooth fitted curves are shown for clarity and comparison.

Tests with NiO

The traction coefficients generated using dry NiO powder as a lubricant are presented in Figs. 4 through 9. The values of τ_0 and τ_l decreased as applied normal loads and increased for all temperatures except 600°F. However, approximate values of τ_l remained almost insensitive to the temperature variation. Also, at higher temperatures the traction curve approached its peak and at a lower value of slip ratio.

The traction curve beyond τ_l decreases as ΔU increases. The decrease in traction coefficient beyond τ_l, up to a limiting value of τ_T, was observed (temperature effect is noted). As seen from the plots of Figs. 4 and 5, τ_T dropped from 0.387 to 0.23 at $\%\Delta U$ equal to 90%.

Tests with TiO_2

The traction coefficients generated using dry TiO_2 powder as a lubricant are presented in Figs. 10 through 15. At room temperature τ_0 and τ_l were lower than those at higher temperatures. However, at 1200°F the traction curve approaches its peak at a higher value of slip ($\%\Delta U$ = 15% and α_1 = 1.77 deg) while at room temperature the corresponding slip values were 10% and its α_1 = 3.5 deg. (Figs. 10 and 11).

The depth of the wear track generated on the test disks was insignificant and immeasurable, although the surface finish was changed about fourfold over the original one. The track width was about 47 mils, 1.7 times that of the calculated Hertz half width (one-half of the major diameter), the center portion of the trace appeared smooth and glassy while the

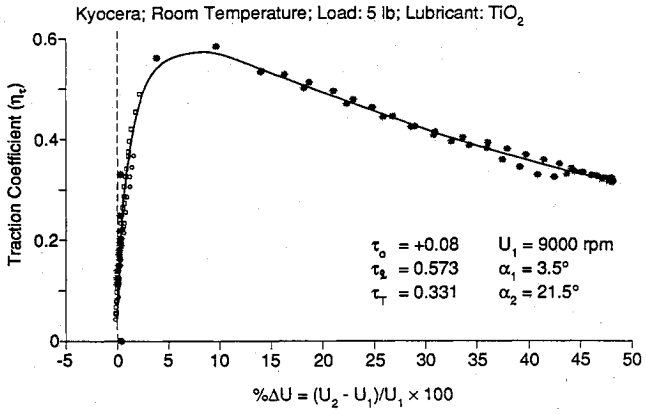

Fig. 10 η_τ vs $\%\Delta U$ for TiO_2 powder at *RT*, *Wn* = 22.23N.

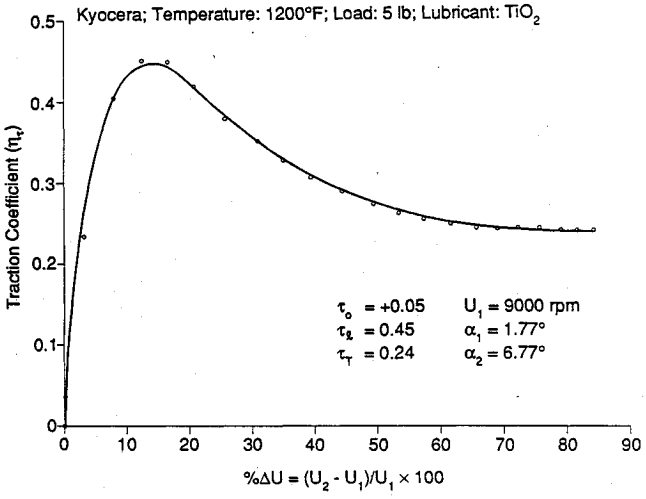

Fig. 11 η_τ vs $\%\Delta U$ for TiO_2 powder at 650°C, *Wn* = 22.23N.

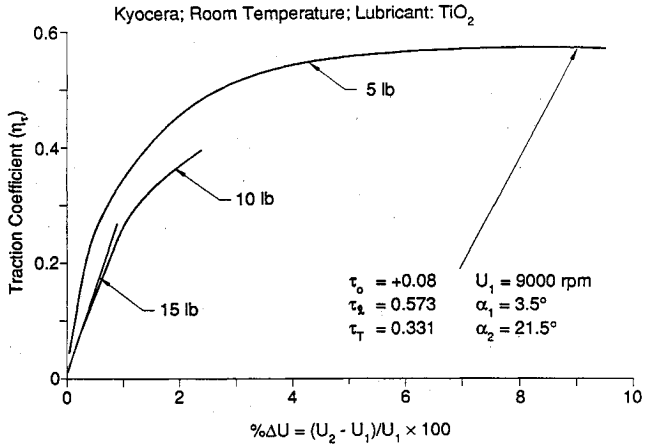

Fig. 12 Traction data for TiO_2 powder at *RT*; *Wn* = 22.23N, 44.48, and 66.72N.

edges were discolored and showed deposition and transferred or adhered powder film. This film of powder which was strongly bonded onto the surface faded outwardly, suggesting a plowing action akin to the side flow in liquid lubrication.

Tests with $ZnMoO_2S_2$

The traction data using $ZnMoO_2S_2$ powder at room temperature are given in Fig. 16 and at 1050°F are given in Fig. 17 for a constant load of 5 lbs. At room temperature τ_0 was higher than that at a high temperature of 1050°F, although τ_l and τ_T were lower than those at higher temperatures. How-

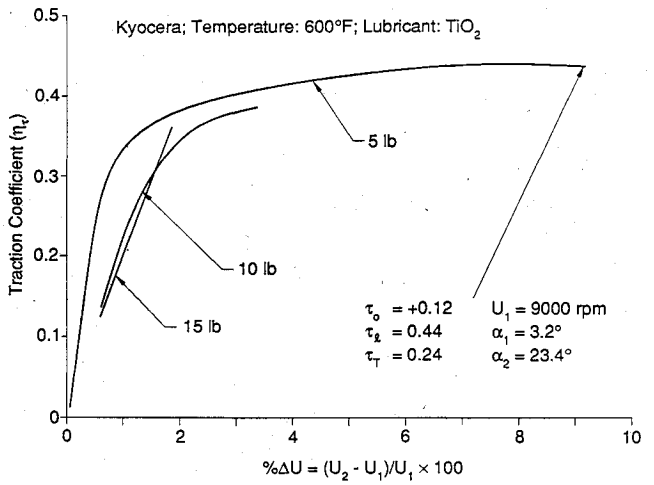

Fig. 13 Traction data for TiO_2 powder at 316°C; *Wn* = 22.23, 44.48 and 66.72N.

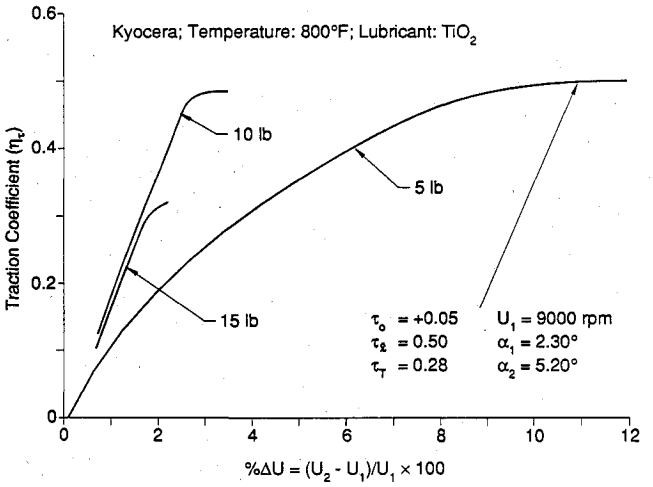

Fig. 14 Traction data for TiO_2 powder at 427°C; *Wn* = 22.23, 44.48, and 66.72N.

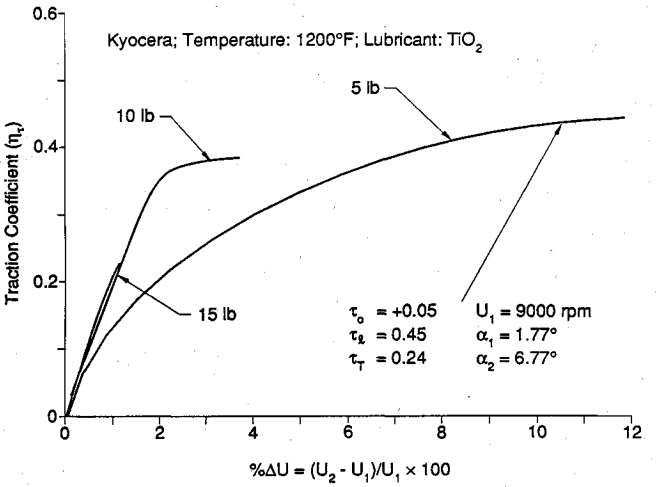

Fig. 15 Traction data for TiO_2 powder at 650°C; *Wn* = 22.23, 44.48, and 66.72N.

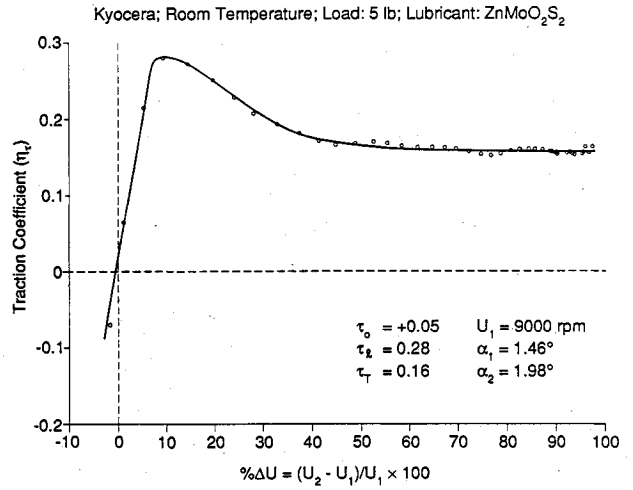

Fig. 16 η_T vs %Δ*U* for $ZnMoO_2S_2$ at *RT*, *Wn* = 22.23N.

ever, at *RT* the traction curve approaches its peak at a lower value of slip (%Δ*U* = 10% and α_1 = 1.46°), while at 1050°F the corresponding slip value was 12% and its α_1 = 1.2 deg.

The traction data at *RT* are given in Fig. 18 for various contact loads. Figure 18 shows a progressive decrease in the τ_l with an increase in load. The same holds for the traction data at 800°F and 1050°F given in Figs. 19 and 20, with the exception at 800°F τ_l for 10 lbs, which has about the same value at τ_l at 5 lbs. Worthy of note, overall traction coefficients show a decrease at 800°F relative to *RT* and 1050°F data. In almost all cases the τ_0 was about zero within the tolerances of the experimental data, which is reminiscent of a liquid lubricant's behavior. The limiting stresses τ_l were also about 50% less than those measured with NiO and TiO_2. At higher temperature, 1050°F and contact stresses beyond 125 ksi, the traction curves began to flatten or rise as slip was increased. This phenomenon is analogous to that of film rupture in liquid lubricants. The appearance of the contact surfaces was similar to that from the TiO_2 tests.

Overall the traction curves with dry $ZnMoO_2S_2$ are reminiscent of liquid lubricants. However, the review of literature[5,6] on liquid lubricant traction curves shows a decrease in η_T beyond the slip ratio of 20%, which is mainly due to thermal effects, while the traction curve for $ZnMoO_2S_2$ begins to flatten or slightly raise rather than drop off.

Unlubricated (Dry) Tests

To provide a baseline for assessing the advantages of powder lubricants, tests were carried out with no insertion of lubricant into the contact. This test was conducted with three different types of Si_3N_4 materials. A sample result at 1200°F is shown in Fig. 21. The dry traction curves showed no change in traction performance with load or temperatures. The traction curves closely resemble friction curves that one might expect from a pin-on-disk apparatus.

As can be seen from the plots of Fig. 21, traction data with TiO_2 were also plotted for comparison. With the contact load of 15 lbs (Hertzian stress = 160 ksi) the traction coefficient approached a value of approximately 0.9 at %Δ*U* ~ 10%, and the η_T has risen to approximately 0.93 at 60% slip ratio as shown in Fig. 21. These values of maximum traction coefficients (about 0.9) correlate well with the static coefficient of friction reported elsewhere for Si_3N_4 materials. In comparison with powder lubricated tests, the results of the dry condition showed the highest values of τ_0, τ_l, and α_2 and wear depth.

Quasi-Hydrodynamic Model

Figure 22 compares the traction curves of dry MoS_2 powder with a 10 weight synthetic traction fluid at room temperature. It can be seen that good agreement between the two curves is obtained up to a slip ratio of 33%. However, the liquid

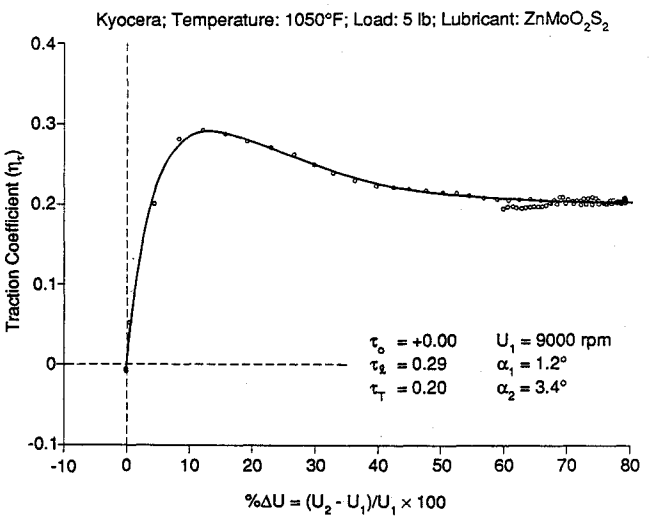

Fig. 17 η_τ vs $\%\Delta U$ for $ZnMo_2S_2$ at 566°C; Wn = 22.23N.

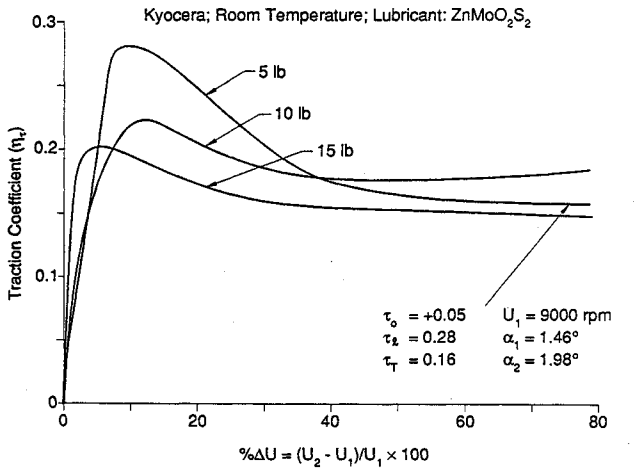

Fig. 18 Traction data for $ZnMoO_2S_2$ powder at *RT*; Wn = 22.23, 44.48, and 66.72N.

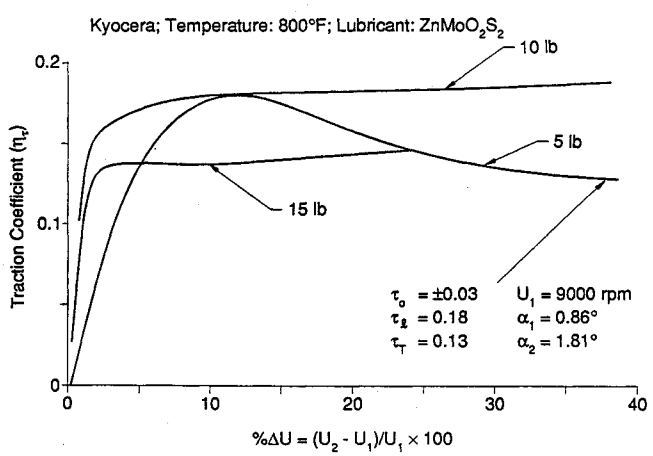

Fig. 19 Traction data for $ZnMoO_2S_2$ powder at 427°C; Wn = 22.23, 44.48, and 66.72N.

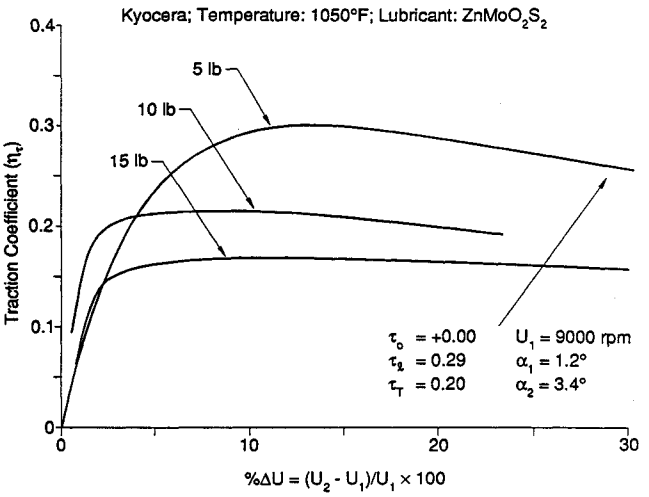

Fig. 20 Traction data for $ZnMoO_2S_2$ powder at 566°C; Wn = 22.23, 44.48, and 66.72N.

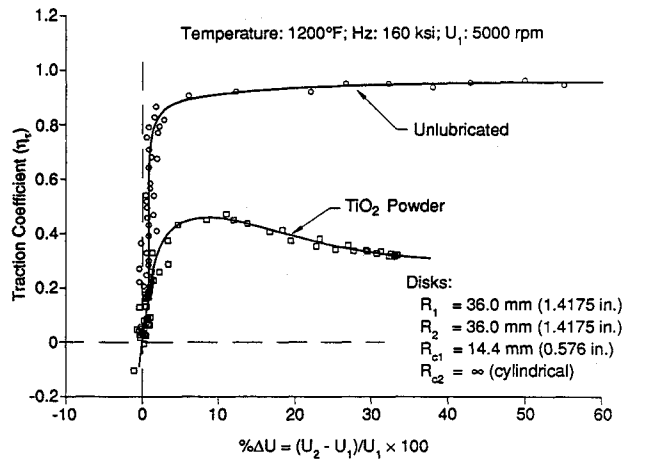

Fig. 21 Traction data for unlubricated and powder TiO_2 lubricated Si_3N_4 materials at 650°C, Wn = 44.48N.

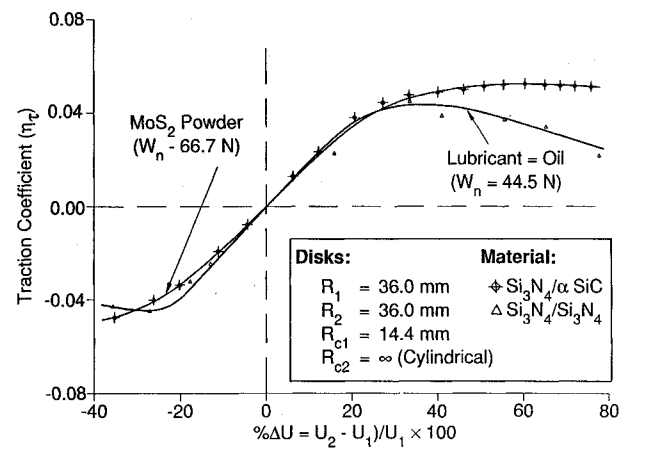

Fig. 22 Traction data for dry MoS_2 powder (Hz = 1.11 GPa) and synthetic fluid equivalent to SAE 10 (Hz − 0.97 GPa) at *RT*, U_1 = 188.5 m/s.

lubricant shows a decrease in η_τ beyond the slip ratio of 33%, which is chiefly due to thermal effects, while the traction curve for MoS_2 begins to flatten rather than drop off.

The results of all powder lubricated series of experiments indicate that the mechanism of powder flow seems to follow some of the basic features of hydrodynamic lubrication by exhibiting a layer-like shear, reminiscent of fluids. This shear is deemed responsible for the reduction in traction coefficients and wear that accompanies the presence of debris between interacting surfaces. The nature of the sheared flow causes the least possible discontinuity between the various laminae of the powder bed. Thus, the basic feature of the quasi-hydrodynamic model is a layered flow of the powder bed, as portrayed in Fig. 23. While powder lubricants are similar to fluids, they do have some unique features, which are discussed below.

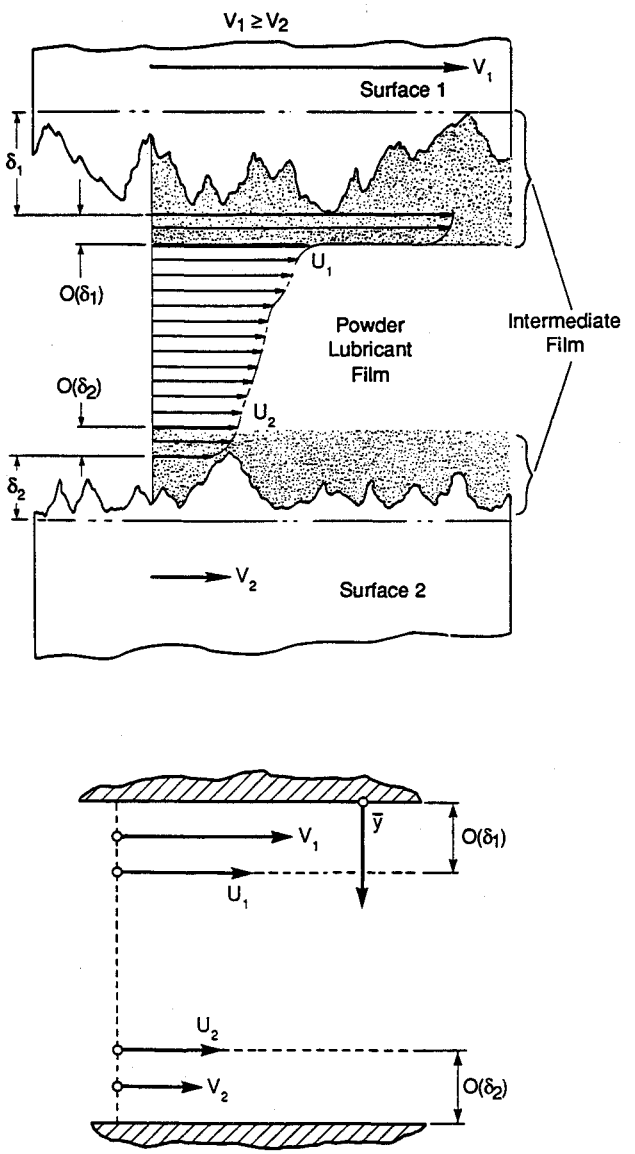

Fig. 23 Quasi-hydrodynamic model for powder lubrication.

Intermediate Film

It has been postulated and is so shown in the model of Fig. 23 that an intermediate film, a form of boundary layer, is created between the interacting surfaces and the lubricant film under powder lubrication conditions. An accommodation of velocities occurs across the intermediate film between the velocities of the two surfaces (V_1 and V_2) and the edge velocities of the lubricant film (U_1 and U_2). The thickness of the intermediate films correspond to the surface roughness (δ_1 and δ_2) of the respective mating material.

The tests conducted under this program clarify and amplify the mechanism of formation of these intermediate films. The result of prolonged exposure to powder lubrication is the formation of this adhesive film, which consists of the powder lubricant or of one of its components, either in pure form or in some chemically altered state, very likely an oxide. Thus, the tribological film formed in powder lubrication resembles the form portrayed schematically in Fig. 23. The intermediate layer, made up of the adhered powder, has the flexibility of behaving either as a solid or as a semi-powder in which considerable creep occurs. This creep makes the accommodation of flow velocities from V_1 and V_2 to U_1 and U_2 possible.

Conclusions

1) The NiO and TiO_2 triboparticulates changed the shapes of the traction curves. Compared with the unlubricated data, the powder reduces the traction coefficients over a wide span of slip ratios. Its effect on lowering the effective contact shear stress, τ_l was about 50% relative to the unlubricated case.

2) The traction characteristics of the $ZnMoO_2S_2$ powder were quite different compared to the NiO and TiO_2 powders. The $ZnMoO_2S_2$ powder gave zero threshold shear stress and low traction coefficients under all test conditions. Overall the behavior of this powder and the magnitude of the traction coefficients were very similar to those seen with liquid lubricants.

3) The persistent presence of powder buildup on the outsides of the contact region suggests the occurrence of side leakage of the powder lubricant, analogous to the sideflow in liquid EHD.

4) Due to the short duration of each test, the amount of wear that took place on the disks was too small to measure accurately. Therefore, the data reported should only be used to compare the traction characteristics of the powder lubricants with the chosen combination of disk materials.

5) Since the traction in solid lubrication is most likely a function of both the disk materials and the powder lubricant, care must be taken about generalizing these data to predicting the behavior of the same lubricants with other disc materials.

Acknowledgments

Acknowledgment is due the United States Air Force Wright Aeronautical Laboratories for its sponsorship of this investigation and in particular to R. Dayton of AFWAL/POSL for his sustained interest in and support of this work. The author gratefully acknowledges D. Hosterman, J. Walton, and A. Soltesz of MTI for their support given at various stages of this effort.

References

[1]Heshmat, H., Pinkus, O., and Godet, M. "On a Common Tribological Mechanism Between Interacting Surfaces," *Society of Tribologists and Lubrication Engineers Transactions*, Vol. 32, No. 1, 1989.

[2]Heshmat, H. "The Rheology and Hydrodynamics of Dry Powder Lubrication," paper presented at the ASME-STLE Tribology Conf., Ontario, Canada, 1990, STLE. Vol. 34, No. 3, 1991, pp. 433–439.

[3]Heshmat, H. "Wear Reduction Systems: Powder Lubricated Piston Rings for Coal Fired Diesel Engines," *Proceedings DOE-METC Contractors' Review Meeting*, Oct. 1989.

[4]Heshmat, H. "Diesel Wear: Powder-Lubricated Piston Rings for Coal-Fired Diesel Engines," *Proceedings DOE-METC Contractors' Review Meeting*, Mar. 1990.

[5]Walowit, J. A., and Anno, J. N. *Modern Development in Lubrication Mechanics*, Applied Science Publishers, Ltd., London, 1975.

[6]Gupta, P. K. "Traction Modeling of Military Oils," Technical Rept. G-104-86-TR, prepared for AFAPL/AFWAL, Jan. 1986.

[7]Heshmat, H., and Dill, J., "Traction Characteristics of High Temperature Powder Lubricated Ceramics ($Si_3N_4/\alpha SiC$)," paper presented at ASME-STLE Tribology Conf., Ontario, Canada, 1990, Trans. of STLE, Vol. 34, No. 4, 1991, pp. 460–466.

[8]Heshmat, H. "The Effect of Dynamic Loads in Tribometers—Analysis and Experiments," *Proceedings of the 16th Leeds-Lyon Symposium on Tribology*, Elsevier Science Publishers, Tribology Series 17, Lyon, France, 1989.